Virtual elements for solids - an engineering perspective

Institut für Kontinuumsmechanik

Leibniz Universität Hannover

Peter Wriggers

Institut für Kontinuumsmechanik
Leibniz Universität Hannover

June 20, 2024

NEMESIS - Workshop 2024, 19.-21. June, Montpellier

Acknowledgement: F. Aldakheel, C. Böhm, B. Hudobivnik, A. Hussein, P. Pimenta, T. P. Wu, B. Xu

Virtual element method (VEM)

Mesh for a crack propagation problem

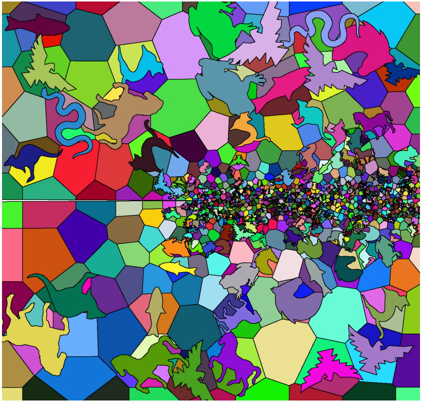

Aldakheel, Hudobivnik & Wriggers (2019)

- **Advantages of virtual elements**
  - Arbitrary number of nodes
  - Non-convex shape
  - $\boldsymbol{u}_h$ only defined at the boundary
  - C^n-continuous ansatz possible
- **Drawbacks:**
  - Stabilization necessary
  - Volume integrals for nonlinear problems

Virtual element method (VEM)

Phasefield solution

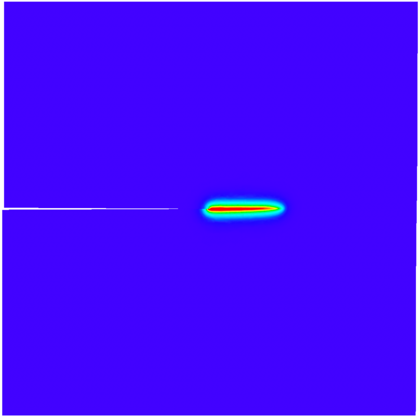

Aldakheel, Hudobivnik & Wriggers (2019)

- **Advantages of virtual elements**
  - Arbitrary number of nodes
  - Non-convex shape
  - $\boldsymbol{u}_h$ only defined at the boundary
  - C^n-continuous ansatz possible
- **Drawbacks:**
  - Stabilization necessary
  - Volume integrals for nonlinear problems

An engineering view: Observations and Requirements

Bending dominated problems

Cook's solid

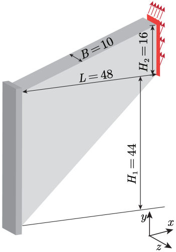

linear solution

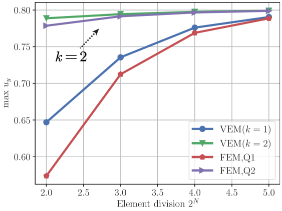

nonlinear solution

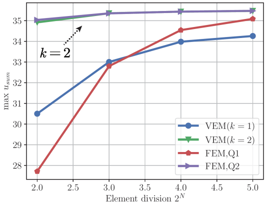

1. Coarse mesh accuracy
   - Higher order elements
   - Special stabliization, see PW et al. 2017
2. Accurate solutions: Adaptivity

An engineering view: Observations and Requirements

Incompressible solids, Punch problem

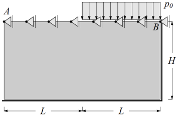

(a) Schematic setup

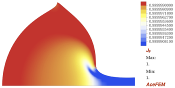

(b) Deformed configuration

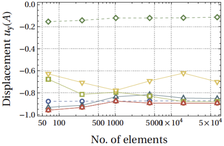

(a) $\nu = 0.499$

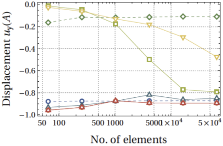

(b) $\nu = 0.49999$

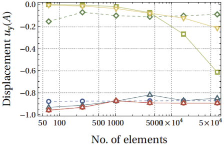

(c) $\nu = 0.4999999$

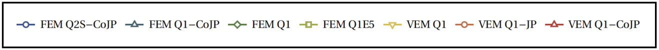

1. Locking free elements
2. Mixed Methods

An engineering view: Observations and Requirements

Anisotropic solids

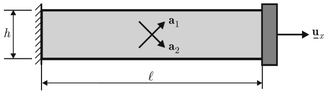

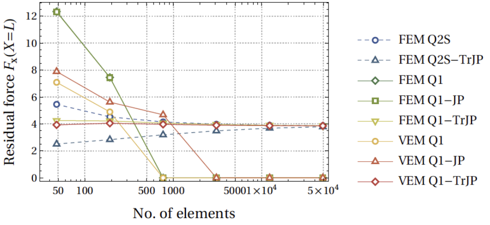

(b) $F_x(X = L)$ versus no. of elements

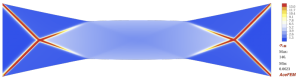

(a) $\alpha_1 = 10^3 \mathrm{N/mm}^2$

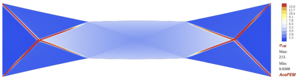

(b) $\alpha_1 = 10^4 \mathrm{N/mm}^2$

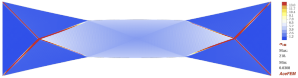

(c) $\alpha_1 = 10^5 \mathrm{N/mm}^2$

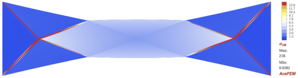

(d) $\alpha_1 = 10^6 \mathrm{N/mm}^2$

An engineering view: Observations and Requirements

Non-smooth problems, Crystal Plasticity

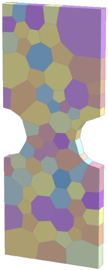

Specimen

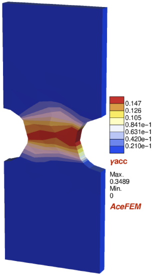

Plot γ_{acc}

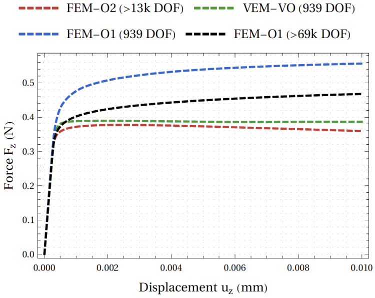

Force – displacement plot

1. Use low (1^{st}) order discretization schemes
2. Locking free elements
3. Special active set algorithms / regularization schemes

Advantages of VEM in Engineering Applications

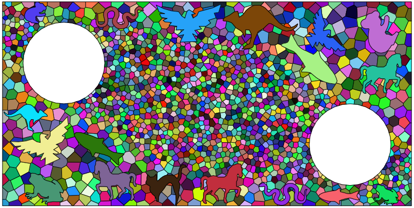

- **Fracture:** New element shapes can be defined during crack propagation
- **Contact:** Node-to-node concept can be used for unstructured meshes
- **Homogenization:** Crystals can be modeled with one virtual element
- **Adaptivity:** Hanging nodes are consistent with VE ansatz
- **Agglomeration:** Badly shaped finite elements can be replaced by VE
- **Element design:** C^1-order "FE" can be easily constructed using VEM
- **Discrete elements:** Flexible particles can be introduced via VEM

Advantages in Engineering Applications

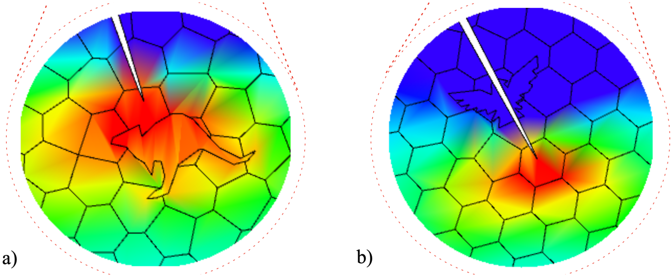

Fracture Mechanics

- New element shapes can be defined during crack propagation

crack path

Advantages in Engineering Applications

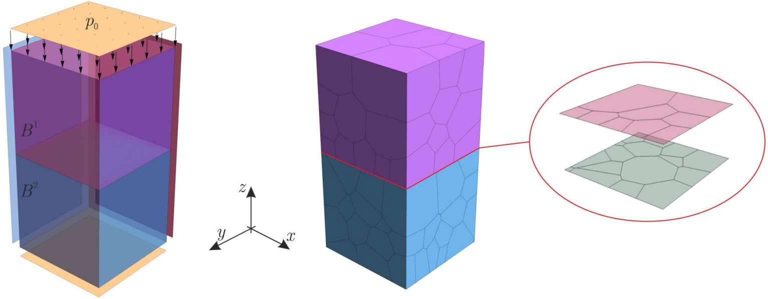

Contact Mechanics

- Node-to-node concept can be used for unstructured meshes

Rotating blocks

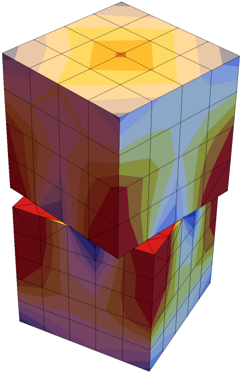

Rotating Blocks

Features

- Large rotation of upper block
- Free edges
- Updated "node-to-node" contact

Contact with VEM in three dimensions

- **Rotating Blocks, Reaction force**

- Comparison of different stabilizations
- $0° - 90°$ $\qquad$ $0° - 360°$

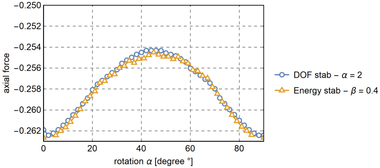

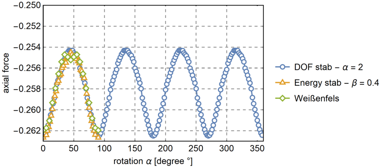

Advantages in Engineering Applications

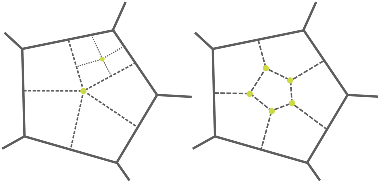

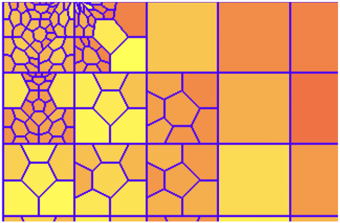

Adaptive Methods

- Hanging nodes are consistent with VE ansatz

Advantages in Engineering Applications

Virtual plate element $\Rightarrow$ "FEM" plate element

Triangular and quadrilateral virtual plate elements

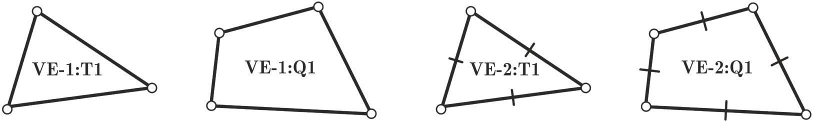

- EL1: 9 and 12 d.o.fs (const. curvature), (VE-1:T1 and VE-1:Q1)
- El 2: 12 and 16 d.o.fs (linear curvature), (VE-2:T1 and VE-2:Q1)
- C^1-continuity with d.o.fs deflection w and rotations $w_{,x}$ and $w_{,y}$
- Can be easily integrated in classical finite element codes

- Square plate under $\bar{q}$, St-1: $\frac{D}{2\,A_e}\sum_{i=1}^{n_V}\left[\widehat{w}(\mathbf{X}_i)^2 + \left\| \frac{L_{i-1}+L_i}{2} \nabla \widehat{w}(\mathbf{X}_i) \right\|^2\right]$

$$\widehat{w}(\mathbf{X}_i) = w_h(\mathbf{X}_i) - \Pi w_h(\mathbf{X}_i)$$

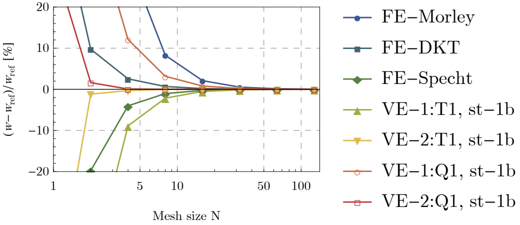

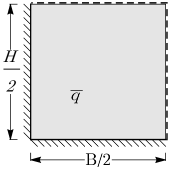

- Square plate under $\bar{q}$, St-2: $\frac{D}{2\,A_e}\sum_{k=1}^{n_E}\frac{1}{L_k}\int_{\Gamma_k}\left[\widehat{w}(\mathbf{X}_k)^2 + \|L_k \nabla \widehat{w}(\mathbf{X}_k)\|^2\right] d\Gamma$

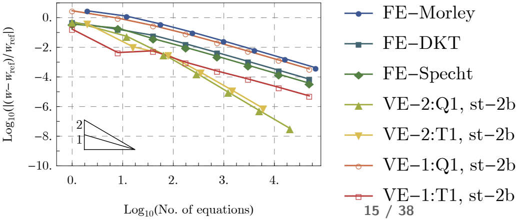

Advantages in Engineering Applications

C^1**-continuous Kirchhoff-Love shells** (Wu, Pimenta, PW 2024)

Shell discretized by flat triangular virtual elements

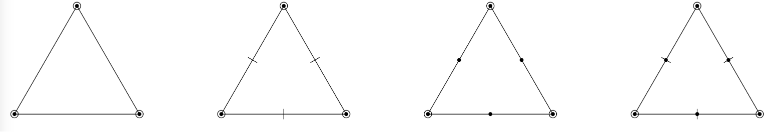

$\mathfrak{E}_1$ $\mathfrak{E}_2$ $\mathfrak{E}_3$ $\mathfrak{E}_4$

1. Deflection: $3^{rd} order$
2. Rotations around edge: 1^{st} and 2^{nd} order
3. In-plane displacements: 1^{st} and 2^{nd} order

$\mathfrak{E}_1 = \{3, 1, 1\}$, $\mathfrak{E}_2 = \{3, 2, 1\}$,$\mathfrak{E}_3 = \{3, 1, 2\}$ and $\mathfrak{E}_4 = \{3, 2, 2\}$

Advantages in Engineering Applications

Kirchhoff-Love shell, Cantilever (Wu, Pimenta, PW 2024)

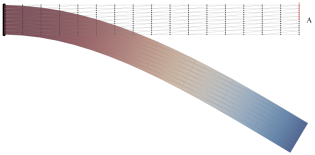

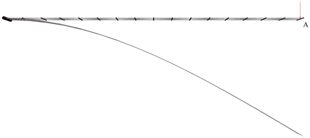

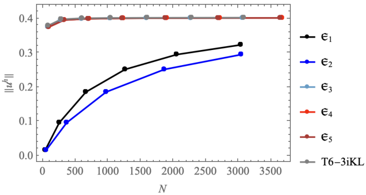

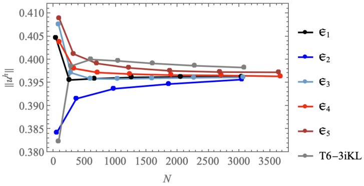

An engineering view: Observations and Requirements

Kirchhoff-Love shell, Z-Profil under torsion (Wu, Pimenta, PW 2024)

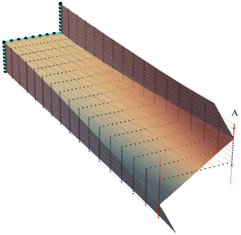

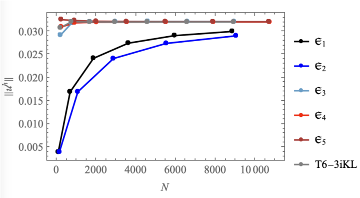

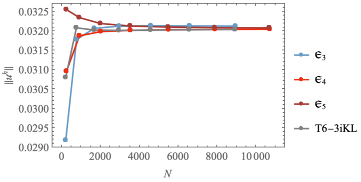

Advantages in Engineering Applications

Kirchhoff-Love shell, pinched sphere (Wu, Pimenta, PW 2024)

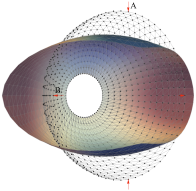

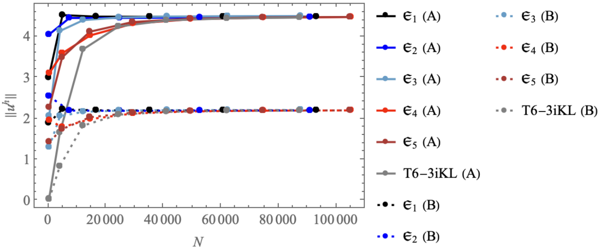

Advantages in Engineering Applications

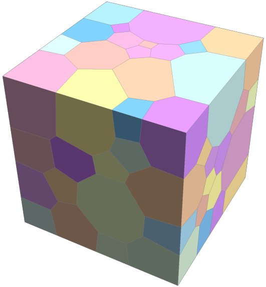

100 polyhedral elements

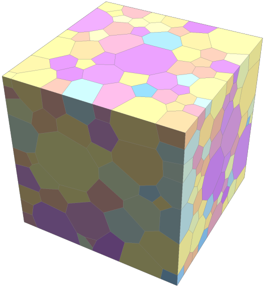

700 polyhedral elements

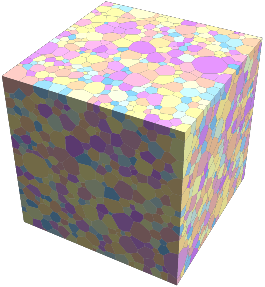

7000 polyhedral elements

Homogenization procedures

- Polycrystals modeled with one VE per grain

Homogenization, effective macroscopic stress field

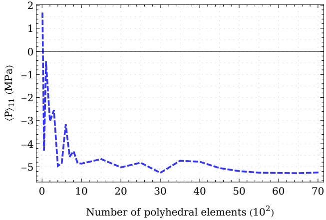

$\langle \boldsymbol{P} \rangle_{11}$

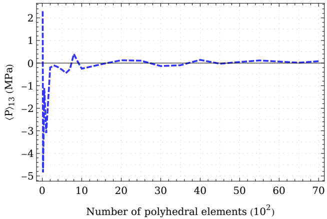

$\langle \boldsymbol{P} \rangle_{13}$

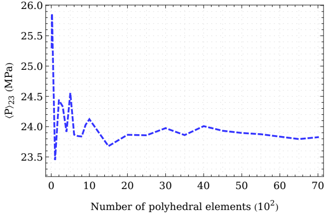

$\langle \boldsymbol{P} \rangle_{23}$

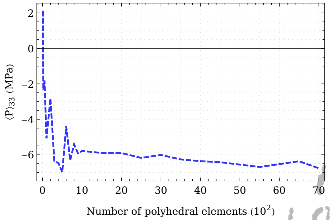

$\langle \boldsymbol{P} \rangle_{33}$

Engineering Application: VEM for Plasticity

Elasto-plasticity

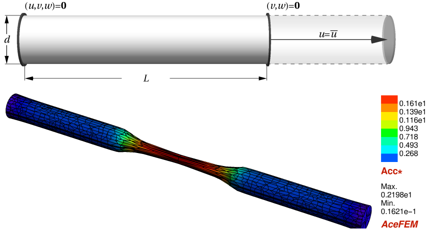

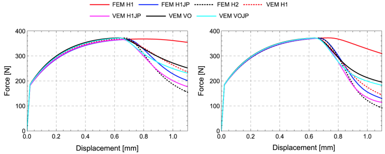

(a) No. elem.=640 **(b)** No. elem.=10000

Necking problem—force-displacement response for two different meshes

Crystal plasticity

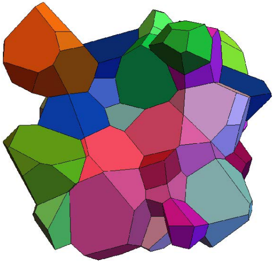

- Low order VEM
- Comparison with FEM (accuracy, efficiency, robustness,...)

Summary: Observations and Requirements

Implications

1. Real world problems need coarse mesh accuracy
2. For non-smooth problems: low order discretization
3. 1^{st} order leads to constant gradients $\rightarrow$ fast
4. For smooth nonlinear applications: second order schemes sufficient
5. Locking free elements (div$u$ =0) $\rightarrow$ mixed methods
6. Locking free elements bending $\rightarrow$ higher order methods
7. Clear choice of stabilization parameters
8. VEM formulations which do not need stabilization

Virtual element method (VEM)

$$V_{h|\Omega_v} = \left\{ \boldsymbol{u}_h \in [H^1(\Omega_v)]^d : \boldsymbol{u}_h|_{\Gamma_e} \in \mathsf{P}_n(\Gamma_e) \, \forall \Gamma_e \in \Gamma_v \, , \Delta \boldsymbol{u}_h \in \mathsf{P}_{n-2}(\Omega_v) \right\}$$

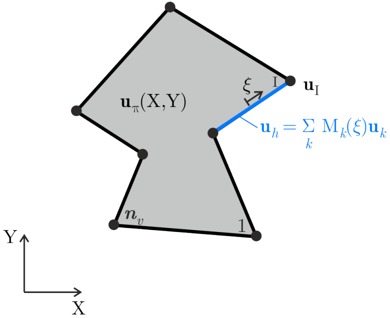

- $\boldsymbol{u}_h$ defined at the boundary Γ_e
- $\boldsymbol{u}_h$ is continuous at all edges $\Gamma_e \in \Gamma_v$
- $\mathbf{u}_I$ is defined at each vertex $\mathbf{X}_I$, vector of all DOF: $\mathbf{u}_v = \bigcup_I^{n_V} \mathbf{u}_I$
- **Projection onto polynomial space**

$$\begin{array}{rcl} \Pi : V_{h|\Omega_v} & \longrightarrow & [\mathsf{P}_n(\Omega_v)]^d \\ \boldsymbol{u}_h & \mapsto & \Pi(\boldsymbol{u}_h) = \boldsymbol{u}_\pi \end{array}$$

- $\boldsymbol{u}_\pi = \mathbf{A}\,[\mathbf{N}_\pi^k]^T \quad \Longleftrightarrow \quad u_{\pi\,i} = A_{ij} N^k_{\pi\,j}$
  $\mathbf{N}_\pi^k = \left(1, X, Y, Z, X^2, XY, \dots, Z^k\right)$
- **The Question**: How to compute A_{ij} and it dependency on the nodal values

$$\mathbf{u}_v \rightarrow \boxed{\boldsymbol{u}_\pi = \mathbf{N}_\pi^k(\mathbf{X})\,\mathbb{P}\,\mathbf{u}_v} \; ?$$

Virtual element method (VEM)

General approach to compute the coefficients A_{ij} of $\mathbf{u}_\pi$:

- Mean values of $\boldsymbol{u}_h$ are equal to the mean values $\boldsymbol{u}_\pi$ on element edges

$$\boxed{\int_{\Gamma_v} \boldsymbol{u}_\pi \, d\Gamma = \int_{\Gamma_v} \boldsymbol{u}_h \, d\Gamma}$$

- Use orthogonality of the gradients of the VEM Ansatz $\boldsymbol{u}_h$ to the projection $\boldsymbol{u}_\pi$

$$\boxed{\int_{\Omega_v} (\nabla \boldsymbol{u}_\pi - \nabla \boldsymbol{u}_h) \cdot \nabla \mathbf{p}^k \, d\Omega = 0}$$

- Does not depend on the weak form $\Rightarrow$ valid for small and large strain cases
- Necessary to compute the integrals
  1. $\int_{\Omega_v} \nabla \boldsymbol{u}_\pi \cdot \nabla \mathbf{p}^k \, d\Omega \longrightarrow \mathbf{G}\, \hat{\mathbf{a}}$
  2. $\int_{\Omega_v} \nabla \boldsymbol{u}_h \cdot \nabla \mathbf{p}^k \, d\Omega \longrightarrow \mathbf{b}(\mathbf{u}_v, \mathbf{m}_v)$

Virtual element method (VEM)

- Equation system

$$\mathbf{G}\,\hat{\mathbf{a}} = \mathbf{b}(\mathbf{u}_v, \mathbf{m}_v) \quad \Rightarrow \quad \hat{\mathbf{a}} = \mathbf{G}^{-1}\,\mathbf{b}(\mathbf{u}_v, \mathbf{m}_v)$$

- Projection for the gradient

$$\boxed{\nabla \boldsymbol{u}_\pi = \hat{\mathbf{A}}\,\nabla \mathbf{N}_\pi^k(\mathbf{X}) = \mathbb{B}_\pi^k(\mathbf{X}) \begin{Bmatrix} \mathbf{u}_v \\ \mathbf{m}_v \end{Bmatrix}}$$

- Complete projection by

$$\int_{\Gamma_v} \boldsymbol{u}_\pi \, d\Gamma = \int_{\Gamma_v} \boldsymbol{u}_h \, d\Gamma \quad \Rightarrow \quad \sum_I^{n_V} \boldsymbol{u}_\pi(\mathbf{X}_I) = \sum_I^{n_V} \mathbf{u}_I$$

which yields the missing constants in $\mathbf{A}$

- Final projection for the displacement

$$\boxed{\boldsymbol{u}_\pi = \mathbf{A}\,\mathbf{N}_\pi^k(\mathbf{X}) = \mathbf{N}_\pi^k(\mathbf{X})\,\mathbb{P}^k \begin{Bmatrix} \mathbf{u}_v \\ \mathbf{m}_v \end{Bmatrix}}$$

Virtual element method (VEM)

Construction of weak from and the potential function

- **Weak form**

$$a(\boldsymbol{u}\,,\boldsymbol{v}) \approx a(\boldsymbol{u}_h\,,\boldsymbol{v}_h)$$

with $\boldsymbol{u}_h = \boldsymbol{u}_\pi + (\boldsymbol{u}_h - \boldsymbol{u}_\pi)$ and $\boldsymbol{v}_h = \boldsymbol{v}_\pi + (\boldsymbol{v}_h - \boldsymbol{v}_\pi)$

$$\boxed{a(\boldsymbol{u}_h\,,\boldsymbol{v}_h) = a_{cons}(\boldsymbol{u}_\pi\,,\boldsymbol{v}_\pi) + a_{stab}(\boldsymbol{u}_h - \boldsymbol{u}_\pi\,,\boldsymbol{v}_h - \boldsymbol{v}_\pi)}$$

- **Potential**

$$U(\boldsymbol{u}) \approx U(\boldsymbol{u}_h) = \mathop{\mathsf{A}}_{v=1}^{N_v} U_v(\boldsymbol{u}_h)$$

with

$$\boxed{U_v(\boldsymbol{u}_h) = U_v^{cons}(\boldsymbol{u}_\pi) + U_v^{stab}(\boldsymbol{u}_h - \boldsymbol{u}_\pi)}$$

Mixed virtual element

Hu-Washizu in pressure and dilatation

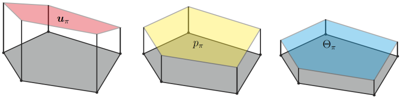

Consistency part

$$U_v^{cons}(\boldsymbol{u}_\pi\,,\Theta_\pi\,,p_\pi) = \int\limits_{\Omega_v} \left[\Psi^{iso}(\boldsymbol{u}_\pi) + \Psi^{p\Theta}(\boldsymbol{u}_\pi\,,\Theta_\pi\,,p_\pi) + \Psi^{dil}(\Theta_\pi)\right]\,\mathrm{d}\Omega$$

with

$$\Psi^{iso}(\boldsymbol{u}_\pi) = \frac{\mu}{2}\left([J_e(\boldsymbol{u}_\pi)]^{-\frac{2}{3}}\,\mathrm{tr}\,[\boldsymbol{b}_e(\boldsymbol{u}_\pi)] - 3\right)$$

$$\Psi^{p\Theta}(\boldsymbol{u}_\pi\,,\Theta_\pi\,,p_\pi) = p_\pi[J_e(\boldsymbol{u}_\pi) - \Theta_\pi]$$

$$\Psi^{dil}(\Theta_\pi) = \frac{K}{4}(\Theta_\pi^2 - 1 - 2\,\ln\Theta_\pi)$$

stabilization only necessary for $\Psi^{iso}(\boldsymbol{u}_\pi)$.

Virtual element method (VEM)

Matrix formulation, 1^{st} order

- Ansatz functions $\boldsymbol{u}_\pi \rightarrow$ linear, $\Theta_\pi\,, p_\pi \rightarrow$ constant
- Deformation gradient: $\boldsymbol{F}_v = \mathbf{1} + \nabla_X \boldsymbol{u}_\pi = \mathbf{1} + \mathbb{B}^1_\pi\, \mathbf{u}_v \rightarrow$ constant
- Left Cauchy-Green tensor: $\Rightarrow \boldsymbol{b}_v(\mathbf{u}_v) = \boldsymbol{F}_v \boldsymbol{F}_v^T \rightarrow$ constant
- Jacobi determinant: $J_e = J_v = \omega_v \,/\, \Omega_v\,,$ $\boxed{\omega_v = \dfrac{1}{n_{dim}} \displaystyle\int_{\gamma_v} (\boldsymbol{X}_v + \boldsymbol{u}_h) \cdot \boldsymbol{n}_v \, \mathrm{d}\gamma}$
- Define $\mathbf{u}_E = \{\mathbf{u}_1\,, \mathbf{u}_2\,, \ldots\,, \mathbf{u}_{nV}\,, \Theta_\pi\,, p_\pi\}$
- Hu-Washizu principle

$$U_v^{cons}(\boldsymbol{u}_\pi\,, \Theta_\pi\,, p_\pi) = \left[\Psi^{iso}(\boldsymbol{u}_\pi) + \Psi^{p\Theta}(\boldsymbol{u}_\pi\,, \Theta_\pi\,, p_\pi) + \Psi^{dil}(\Theta_\pi)\right] \Omega_v$$

- Element residual and tangent follow automatically by employing *AceGen:*

$$\mathbf{R}_v^{cons} = \Omega_v \, \frac{\partial \sum \Psi(\mathbf{u}_E)}{\partial \mathbf{u}_E} \qquad \text{and} \quad \mathbf{K}_{Tv}^{cons} = \frac{\partial \mathbf{R}_v^{cons}(\mathbf{u}_E)}{\partial \mathbf{u}_E}$$

1^{st} order virtual element

Clamped patch (Böhm et al. 2023)

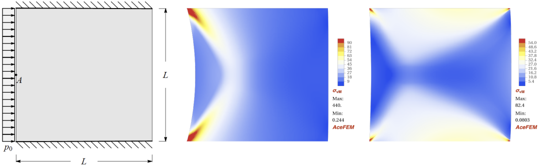

(a) Schematic setup (b) σ_{vM} for $\nu = 0.3$ (c) σ_{vM} for $\nu = 0.499$

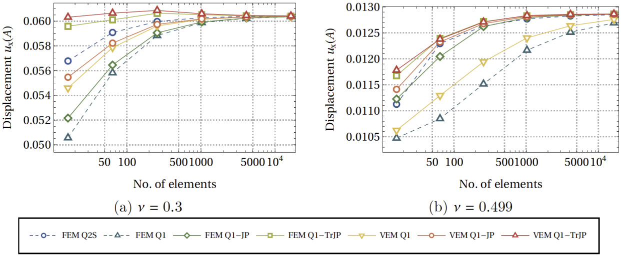

(a) $\nu = 0.3$ (b) $\nu = 0.499$

Virtual element method (VEM)

Matrix formulation, 2^{nd} order

- Ansatz functions $\boldsymbol{u}_\pi \rightarrow$ quadratic
- Define $\mathbf{u}_E = \{\mathbf{u}_1\,, \mathbf{u}_2\,, \ldots\,, \mathbf{u}_{nV}\,, \mathbf{m}_1\,, \ldots\,, \mathbf{m}_{nM}\}$
- Deformation gradient: $\boldsymbol{F}_v = \mathbf{1} + \nabla_X \boldsymbol{u}_\pi = \mathbf{1} + \mathbb{B}^2_\pi(\mathbf{X})\,\mathbf{u}_E$
- Right Cauchy-Green tensor: $\Rightarrow \boldsymbol{C}_v(\mathbf{u}_E) = \boldsymbol{F}_v^T \boldsymbol{F}_v$
- Jacobi determinant: $J_v = \det \boldsymbol{F}_v$
- Potential

$$U_v^{cons}(\boldsymbol{u}_\pi) = \int_{\Omega_v} \Psi(\boldsymbol{u}_\pi)\,\mathrm{d}\Omega$$

- Strain energy function, Neo Hooke

$$\Psi(\boldsymbol{u}_\pi) = \frac{\Lambda}{4}(J_v^2 - 1 - 2\,\ln J_v) + \frac{\mu}{2}(\mathrm{tr}\,\boldsymbol{C}_v - 3 - 2\,\ln J_v)$$

Virtual element method (VEM)

2^{nd} order virtual element

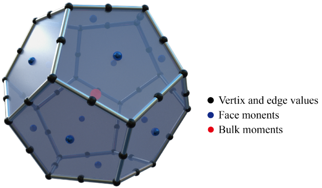

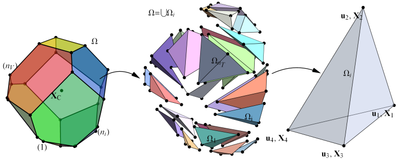

- Integration of potential using subtriangularization
- Element residual and tangent follow automatically by employing *AceGen:*

$$\mathbf{R}_v^{cons} = \Omega_v \, \frac{\partial \sum \Psi(\mathbf{u}_E)}{\partial \mathbf{u}_E} \qquad \text{and} \quad \mathbf{K}_{Tv}^{cons} = \frac{\partial \mathbf{R}_v^{cons}(\mathbf{u}_E)}{\partial \mathbf{u}_E}$$

- Stabilization using *dofi-dofi* with

$$\alpha = \frac{4}{9} \mathrm{tr} \left[\frac{\partial^2 \Psi}{\partial \boldsymbol{C} \, \partial \boldsymbol{C}} \right]$$

2^{nd} order virtual element

Block under compression (Xu, Fan, PW

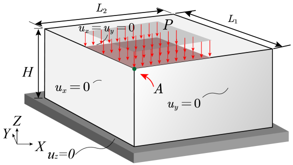

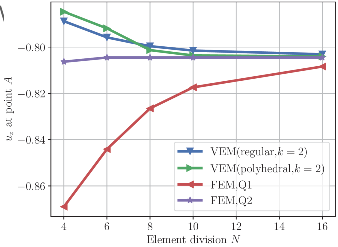

Meshes, deformation and shear stress

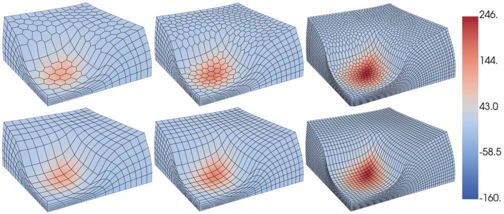

$N = 6$ $N = 8$ $N = 16$

2^{nd} order virtual element

Torsion of a column (Xu, Fan, PW 2024)

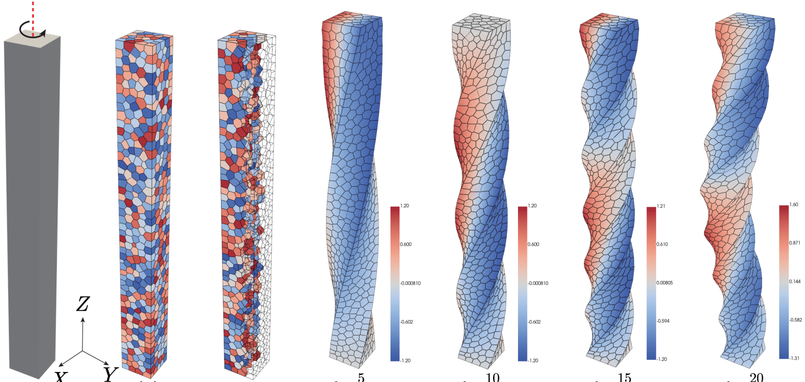

$\theta = \frac{5}{3}\pi$ $\theta = \frac{10}{3}\pi$ $\theta = \frac{15}{3}\pi$ $\theta = \frac{20}{3}\pi$

Torsion

2^{nd} order virtual element

Torsion of a column with slits (Xu, Fan, PW 2024)

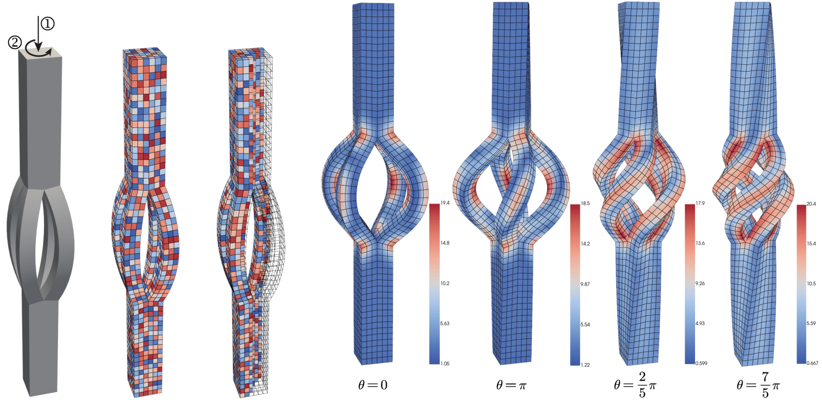

Torsion-Slit

2^{nd} order virtual element

Stresses in a cracked pipe (Xu, Fan, PW 2024)

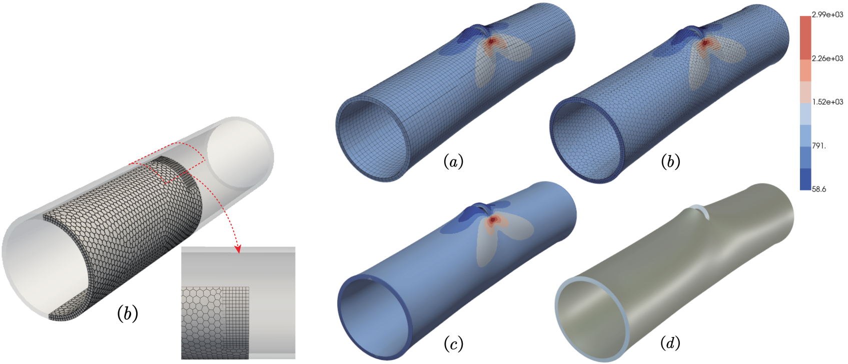

2^{nd} order virtual element

Deformation of a thick shell (Xu, Fan, PW 2024)

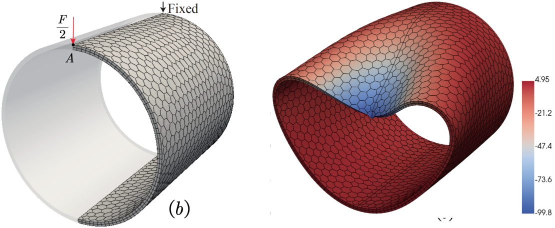

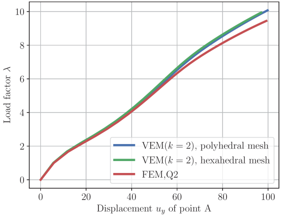

Bibliography

[1] P. Wriggers, B. Reddy, W. Rust, and B. Hudobivnik, "Efficient virtual element formulations for compressible and incompressible finite deformations," *Computational Mechanics*, vol. 60, pp. 253–268, 2017.

[2] M. Cihan, B. Hudobivnik, F. Aldakheel, and P. Wriggers, "3d mixed virtual element formulation for dynamic elasto-plastic analysis," *Computational Mechanics*, vol. 68, pp. 1–18, 2021.

[3] C. Böhm, L. Munk, F. Hudobivnik, B.. Aldakheel, J. Korelc, and P. Wriggers, "Virtual elements for computational anisotropic crystal plasticity," *Computer Methods in Applied Mechanics and Engineering*, vol. 405, p. 115835, 2023.

[4] B. Xu, W.-L. Fan, and P. Wriggers, "High-order 3D virtual element method for linear and nonlinear elasticity," *Computer Methods in Applied Mechanics and Engineering*, p. submitted, 2024.

[5] T. Wu, P. Pimenta, and P. Wriggers, "On triangular virtual elements for Kirchhoff-Love shells," *Archive of Applied Mechanics*, 2024.